EFFECTS OF EMITTER AND RECEIVER MOTION ON ACOUSTIC COHERENCE IN SHALLOW WATER

A Sazontov Institute of Applied Physics, Russian Academy of Science, Nizhny Novgorod
N Vdovicheva Institute of Applied Physics, Russian Academy of Science, Nizhny Novgorod

1. INTRODUCTION

The shallow water acoustic propagation is known to have rather specific features that are not encountered in deep-water waveguides: the sound interactions with lossy bottom lead to the decay of the average wavefield intensity and modify essentially the behaviour of the mutual coherence function (MCF) in comparison with the deep-water situation.

In recent papers [1–4] stochastic transmission in a shallow channel has been studied by formulating a theory in terms of acoustic normal modes, with emphasis on the second and fourth moments of the pressure field produced by a fixed source and registered by a fixed receiver.

For many practical applications there is a need to take into consideration the effects of the source/receiver motion. It is well known that moving source and/or receiver result in a Doppler shift in wavenumber, affecting the modal interference pattern. The significance of the Doppler shift for sonar processing is well established, and the issue of modeling and understanding the complications introduced by the waveguide has received some attention in the literature (see, e.g., [5–8]). These earlier works focused on the source/receiver dynamics in deterministic waveguides. For random shallow water channels the results concerning the effects of the source/receiver motion on acoustic coherence are not available (exception is the work by Uscinski [9] who studied source/receiver dynamics when only one path of multipath configuration is treated). Thus, the latter situation merits a detailed study.

The present report addresses the prediction of acoustic coherence (incorporating both source and receiver motion) in a shallow water environment in which fluctuation phenomena are caused predominantly by fully developed wind seas. We formulate the governing equations for the multimodal MCF of the Doppler-shifted field and present the calculations of the expected total average acoustic intensity and two-point coherence function.

2. FORMULATION OF THE PROPAGATION MODEL

Consider a shallow water channel, in which the background speed of sound $c(z)$ is a function of depth z only. Assume that the sound scattering is caused mainly by a statistically rough and acoustically soft boundary $z = \eta(\mathbf{r}, t)$. Here, $\mathbf{r} = (x, y)$ is the horizontal two-dimensional position vector and t is the time. (The coordinate system is chosen with the z axis downward). The perturbation η is assumed to be a random Gaussian homogeneous and stationary field with zero mean and can be fully described by its autocorrelation function B_η: $B_\eta(\boldsymbol{\rho}, \tau) = < \eta(\mathbf{r}, t)\, \eta(\mathbf{r} + \boldsymbol{\rho}, t + \tau) >$, where the angular brackets $< \cdots >$ indicate ensemble averaging.

Effects of Emitter and Receiver Motion - A Sazontov, N Vdovicheva.

Let a harmonic point source of the time dependence $\exp(-i\omega_0 t)$, where $\omega_0 = 2\pi f_0$ denotes the radian carrier frequency, be located at depth z_0 and move with a constant horizontal velocity vector $\mathbf{u}_s$. The emitted signal passed through a medium with a randomly distributed rough surface is registered by a receiver located at depth z. In a general case, the receiver is moving horizontally with velocity vector $\mathbf{u}_r$. As we will see later, once the expression for the field is found for the moving source, it is straightforward modified to incorporate the receiver motion.

The complex envelope of the acoustic pressure field $P(\mathbf{r}, z, t)$ in an irregular oceanic channel far enough from a moving source can be formally represented by

$$P(\mathbf{r}, z, t) = \int_{-\infty}^{\infty} d\omega\, e^{-i\omega t} \sum_{n=1}^{M(\omega)} P_n(\mathbf{r}, \omega, t)\, \varphi_n(z, \omega). \tag{1}$$

Here, $\varphi_n(z,\omega)$ denotes the n-th vertical eigenfunction of the deterministic background medium corresponding to the eigenvalue κ_n^2 and M is the number of the propagation modes. Each normal mode is modulated by a random amplitude $P_n(\mathbf{r},\omega,t)$ indicating the effect of the surface on acoustic propagation. In the framework of the small-waveheight theory of surface scattering one obtains the following set of coupled mode equations for $P_n(\mathbf{r},\omega,t)$:

$$\left(\frac{\partial^2}{\partial x^2} + \frac{\partial^2}{\partial y^2} + \kappa_n^2(\omega)\right) P_n(\mathbf{r},\omega,t) = -\sum_{m=1}^{M} \eta_{nm}(\mathbf{r},\omega,t) P_m(\mathbf{r},\omega,t) + \varphi_n(z_0,\omega) f(\mathbf{r},\omega). \tag{2}$$

Here, $\eta_{nm}(\mathbf{r},t)$ is the coupling coefficient that is defined, according to [10], as

$$\eta_{nm}(\mathbf{r},\omega,t) = \varphi_n'(0,\omega)\varphi_m'(0,\omega)\,\eta(\mathbf{r},t),$$

where the prime denotes differentiation with respect to depth z and the function

$$f(\mathbf{r},\omega) = \frac{1}{2\pi}\int_{-\infty}^{\infty} dt\, \delta(\mathbf{r} - \mathbf{u}_s t) e^{i(\omega-\omega_0)t}$$

describes the source distribution at angular frequency ω. Equation (2) is the starting equation for the subsequent statistical analysis.

The quantity of ultimate interest is the second moment of the complex pressure:

$$B_p(\mathbf{r}_1, z_1, t_1 | \mathbf{r}_2, z_2, t_2) = < P(\mathbf{r}_1, z_1, t_1)\, P^*(\mathbf{r}_2, z_2, t_2) > . \tag{3}$$

Inserting Eq. (1) into Eq. (3), one finds that

$$B_p(\mathbf{r}_1, z_1, t_1 | \mathbf{r}_2, z_2, t_2) = \int_{-\infty}^{\infty} d\omega_1 \int_{-\infty}^{\infty} d\omega_2\, \Gamma(\cdot|\cdot)\, e^{-i\omega_1 t_1 + i\omega_2 t_2}, \tag{4}$$

where $\Gamma(\mathbf{r}_1, z_1, \omega_1, t_1 | \mathbf{r}_2, z_2, \omega_2, t_2)$ is the total MCF defined as

$$\Gamma(\mathbf{r}_1, z_1, \omega_1, t_1 | \mathbf{r}_2, z_2, \omega_2, t_2) = \sum_{n,m} \Gamma_{nm}(\mathbf{r}_1, \omega_1, t_1 | \mathbf{r}_2, \omega_2, t_2) \varphi_n(z_1, \omega_1) \varphi_m(z_2, \omega_2);$$

$$\Gamma_{nm}(\mathbf{r}_1, \omega_1, t_1 | \mathbf{r}_2, \omega_2, t_2) = < P_n(\mathbf{r}_1, \omega_1, t_1)\, P_m^*(\mathbf{r}_2, \omega_2, t_2) > . \tag{5}$$

For most oceanic applications the characteristic correlation length l_η of surface irregularities is much less than the typical mode cycle distance Λ_n, i.e., $l_\eta \ll \Lambda_n$. In this case, elementary acts of scattering occur at statistically independent ensembles of the surface [11]. As a consequence, we get

$$\Gamma_{nm}(\mathbf{r}_1,\omega_1,t_1|\mathbf{r}_2,\omega_2,t_2) = <P_n(\mathbf{r}_1,\omega_1,t_1)><P_m^*(\mathbf{r}_2,\omega_2,t_2)>, \quad n \neq m,$$

where $<P_n(\mathbf{r},\omega,t)>$ is the coherent field of the n-th mode. As a result, the interference structure of the acoustic field is fully determined by the coherent component of the propagating radiation. Thus, under the assumption made, the second moment of the modal coefficients Γ_{nm} appearing in Eq. (5) becomes

$$\Gamma_{nm}(1,2) = <P_n(1)><P_m^*(2)> + [\Gamma_{nn}(1,2) - <P_n(1)><P_n^*(2)>]\,\delta_{nm}, \tag{6}$$

where $\Gamma_{nn}(1,2)$ is the self-modal MCF. The labels 1 and 2 refer to two different horizontal positions, times and frequencies.

Then, for a slow moving source, for which the source velocity u_s is much smaller than all modal group velocities v_n, i.e., $u_s \ll \min v_n$, the effects such as frequency dependence of mode shape and modal cutoff can be ignored as in the regular case [5–8]. This circumstance together with Eq. (6) permit us to express the second moment of the complex pressure of interest as

$$B_p(\mathbf{r}_1,z_1,t_1|\mathbf{r}_2,z_2,t_2) = <P(\mathbf{r}_1,z_1,t_1)><P^*(\mathbf{r}_2,z_2,t_2)> + B_p^i(\mathbf{r}_1,z_1,t_1|\mathbf{r}_2,z_2,t_2). \tag{7}$$

Here, $<P(\mathbf{r},z,t)>$ is the time domain representation for the coherent component of the total acoustic wavefield that is determined by the expression:

$$<P(\mathbf{r},z,t)> = e^{-i\omega_0 t}\sum_{n=1}^{M} <P_n(\mathbf{r},t)>\,\varphi_n(z,\omega_0),$$

$$<P_n(\mathbf{r},t)> = -\frac{i}{\sqrt{8\pi r(t)}}\sum_{n=1}^{M}\frac{\varphi_n(z_0,\omega_0)}{\sqrt{\kappa_n(\omega_0)}}\,e^{i\kappa_n^d(\omega_0)r(t) - \frac{1}{2}\sigma_n^s(\omega_0)r(t) - i\pi/4}, \tag{8}$$

where $r(t) = |\mathbf{r} - \mathbf{u}_s t|$, $\kappa_n^d(\omega_0) = \kappa_n(\omega_0)\,[1 + (u_s/v_n)\cos\theta_s(t)]$ is the wavenumber Doppler shift, $\theta_s(t)$ is the angle between velocity vector $\mathbf{u}_s$ and the radial vector $\mathbf{r}(t)$ connecting source and receiver, and σ_n^s is the mode scattering coefficient specified below. In the absence of random scattering, when $\sigma_n^s = 0$, Eq. (8) becomes identical to the expressions derived by Guthrie *et al* [5] and Hawker [6] for this special case. The quantity $B_p^i(\mathbf{r}_1,z_1,t_1|\mathbf{r}_2,z_2,t_2)$ entering Eq. (7) is the incoherent part of the total MCF:

$$B_p^i(\mathbf{r}_1,z_1,t_1|\mathbf{r}_2,z_2,t_2) = \sum_{n=1}^{M}[\Gamma_n(\mathbf{r}_1,t_1|\mathbf{r}_2,t_2) - <P_n(\mathbf{r}_1,t_1)><P_n^*(\mathbf{r}_2,t_2)>]\varphi_n(z_1,\omega_0)\varphi_n(z_2,\omega_0), \tag{9}$$

where

$$\Gamma_n(\mathbf{r}_1,t_1|\mathbf{r}_2,t_2) = \int_{-\infty}^{\infty} d\omega_1 \int_{-\infty}^{\infty} d\omega_2\,\Gamma_{nn}(\mathbf{r}_1,\omega_1,t_1|\mathbf{r}_2,\omega_2,t_2)\,e^{-i\omega_1 t_1 + i\omega_2 t_2}. \tag{10}$$

In order to evaluate $\Gamma_n(\mathbf{r}_1, t_1|\mathbf{r}_2, t_2)$ it is most convenient to introduce new coordinates associated with the moving source: $\mathbf{r}' = \mathbf{r} - \mathbf{u}_s t$. Note that in this coordinate system the source is fixed and the medium is moving with a constant velocity $-\mathbf{u}_s$.

We define sum and difference variables as

$$t = 0.5\,(t_1 + t_2)\,,\ \tau = t_1 - t_2,\ \mathbf{r}' = 0.5\,(\mathbf{r}_1' + \mathbf{r}_2') \equiv \mathbf{r} - \mathbf{u}_s t,\ \boldsymbol{\rho}' = \mathbf{r}_1' - \mathbf{r}_2' \equiv \boldsymbol{\rho} - \mathbf{u}_s \tau,$$

with $\mathbf{r} = 0.5\,(\mathbf{r}_1 + \mathbf{r}_2)$ and $\boldsymbol{\rho} = \mathbf{r}_1 - \mathbf{r}_2$. In terms of the new coordinates the self-modal MCF $\Gamma_n(\mathbf{r}_1', t_1|\mathbf{r}_2', t_2) \equiv \Gamma_n(\mathbf{r}', \boldsymbol{\rho}', \tau)$ depends parametrically on t solely through the temporal variations of $\mathbf{r}'$.

Now we define the transverse MCF $\Gamma_n^{\perp}(\cdot)$ as

$$\Gamma_n(\mathbf{r}', \boldsymbol{\rho}', \tau) = e^{i\kappa_n^d(\omega_0)\rho' \sin\alpha}\, \Gamma_n^{\perp}(\mathbf{r}', \rho_{\perp}', \tau), \tag{11}$$

where α is the angle between the vector $\boldsymbol{\rho}'$ and the normal to $\mathbf{r}'$ and $\rho_{\perp}' = \rho' \cos\alpha$.

In what follows we will be interested in the behaviour of $\Gamma_n^{\perp}(\cdot)$ for $r' > 0$ and, subsequently, will account for the source by a matching procedure. Under a rather general condition, the equation governing the change of $\Gamma_n^{\perp}(\cdot)$ as a result of random surface scattering can be derived from the Bethe–Salpeter equation under the forward-scattering approximation (see, e.g., [10]) and has the form

$$\left[\frac{\partial}{\partial r'} + \frac{1}{r'} + \frac{\rho_{\perp}'}{r'}\frac{\partial}{\partial \rho_{\perp}'} + \sigma_n^a\right] \Gamma_n^{\perp}(r', \rho_{\perp}', \tau) = -\sigma_n^s\, \Gamma_n^{\perp}(r', \rho_{\perp}', \tau) + \sum_{m=1}^{M} a_{nm}(\rho_{\perp}', \tau)\, \Gamma_n^{\perp}(r', \rho_{\perp}', \tau), \tag{12}$$

where σ_n^a is the modal attenuation resulting from sediment absorption and $\sigma_n^s = \sum_{m=1}^{M} a_{nm}(0,0)$ is the scattering coefficient. The coupling matrix $a_{nm}(\rho, \tau)$ is given by the expression

$$a_{nm}(\rho, \tau) = \frac{\pi}{2}\, \frac{[\varphi_n'(0)\varphi_m'(0)]^2}{\kappa_n \kappa_m} \int_{-\infty}^{\infty} d\Omega\, e^{-i\Omega\tau} \int_{-\infty}^{\infty} d\text{æ}_y\, e^{i\text{æ}_y \rho}\, F_{\eta}\,(\kappa_n - \kappa_m, \text{æ}_y, \Omega)\,,$$

where $F_{\eta}(\text{æ}, \Omega)$ is the Fourier transform of the surface autocorrelation function $B_{\eta}(\rho, \tau)$ with respect to ρ and τ. At $\mathbf{u}_s = 0$, an equation similar to Eq. (12), but without transverse ρ dependence and subbottom attenuation, was derived by Beilis and Tappert [12] using a parabolic approximation. At this stage, the dependence of $\varphi_n(z)$ and κ_n on argument ω_0 has been omitted for brevity.

In addition to (12), an initial condition in r' must be imposed. This condition, dictated by the harmonic point source, may be obtained by a matching procedure to give

$$\Gamma_n^{\perp}(r', \rho_{\perp}', \tau)\big|_{r'=0} = \frac{\varphi_n^2(z_0, \omega_0)}{8\pi\kappa_n(\omega_0)}\, \delta(\rho_{\perp}') \equiv \frac{\varphi_n^2(z_0, \omega_0)}{8\pi\kappa_n(\omega_0)}\, \delta(\rho_{\perp} - u_{s\perp}\tau), \tag{13}$$

where $u_{s\perp}$ is the velocity component perpendicular to $\mathbf{r}'$. The relations (7)–(13) allow for estimation of the key correlation characteristics of the acoustic signal produced by a moving source in a random shallow water channel.

Until now,we have discussed the formulation in application to a fixed receiver. The general expressions presented above can be straightforward modified to include the receiver motion. It is clear that

Eq. (8) represents the mean field at all range vectors $\mathbf{r}$. Thus, the range vector for a receiver at position $\mathbf{r}_0$ at time $t = 0$ and moving with velocity vector $\mathbf{u}_r$ is given by $\mathbf{r} = \mathbf{r}_0 + \mathbf{u}_r t$ which, being inserted into Eq. (8) yields formally the same expression with the only difference: $r(t)$ must be replaced by

$$r(t) = |\mathbf{r}_0 + (\mathbf{u}_r - \mathbf{u}_s)\, t|. \tag{14}$$

Similarly, once the solution of Eq. (12) is found, the quantity r' must be replaced by (14) and ρ' by $\rho + (\mathbf{u}_r - \mathbf{u}_s)\, \tau$.

3. NUMERICAL CALCULATIONS AND RESULTS

To illustrate the effects of random surface scattering on acoustic transmission we consider the shallow water environment and assume the Pierson–Moskowitz spectrum for $F_\zeta(æ, \Omega)$:

$$F_\eta(æ, \Omega) = \frac{8.1 \times 10^{-3}}{4\pi}\, æ^{-4} \exp\left(-0.74 \frac{g^2}{æ^2 v^4}\right) \delta\left(\Omega - \sqrt{g æ}\right),$$

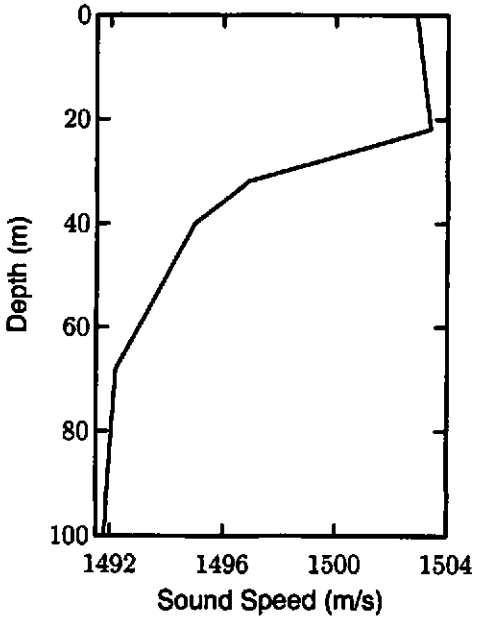

Fig. 1. Sound speed profile chosen for our calculations

where g is the acceleration of gravity and v is the wind speed over the ocean surface.

The sound-speed profile chosen for our calculations is shown in Fig. 1. The environment selected consists of a water column of depth 100 m, with a downward-refracting summer profile, and a homogeneous limestone bottom, with the compressional speed of 1750 m/s, shear speed of 115 m/s, and density of 2 g/cm^3. The water is assumed to be lossless, whereas the attenuation in limestone are assumed to be 0.2 dB/λ for compressional speed and 1.5 dB/λ for shear speed.

The calculations presented below will be carried out for the source frequency of 250 Hz, source depth of 75 m, receiver depth of 55 m, and wind speed of 10 m/s.

3.1 Mean Intensity Behaviour

We begin with observing the effects of rough surface scattering and source/receiver dynamics on the mean intensity as a function of range and depth. We will consider the case where both source and receiver are propagating with the same speed and direction. We assume the source and receiver to be moving along the same track at the speed of 10 m/s.

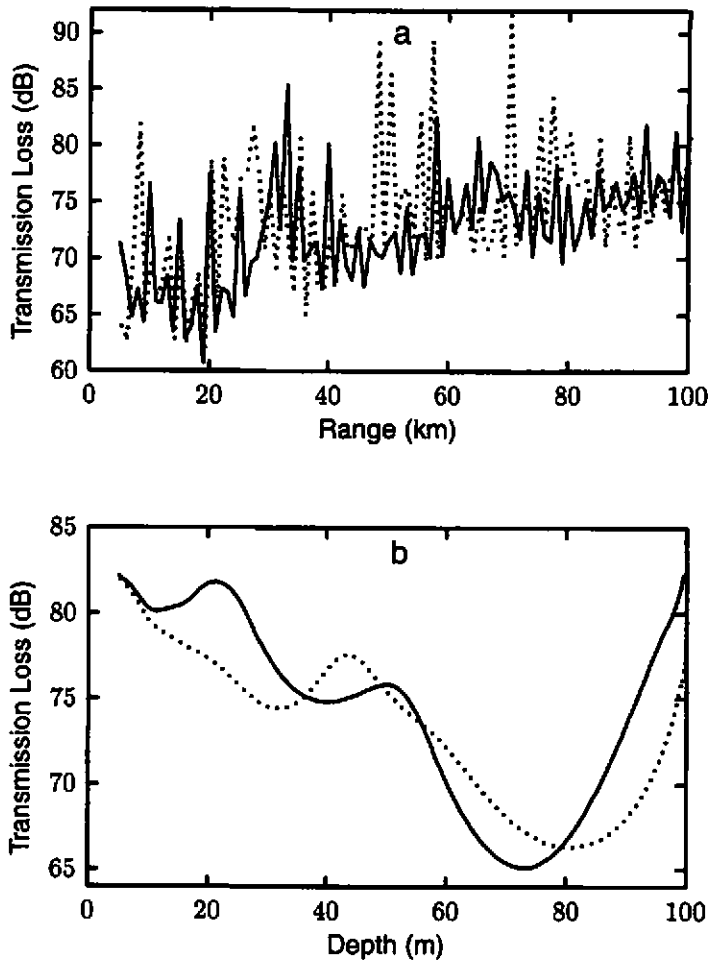

Fig. 2. Transmission loss versus range (a) and depth (b) for source and receiver both moving at 10 m/s (solid curve) and for stationary source and receiver (dotted curve)

In Fig. 2a we plot transmission loss (in decibel notation) versus range as a solid curve. The corresponding result for the static case is indicated by the dotted curve. The interpretation of this figure is quite informative: the joint motion results in a Doppler shift in wavenumber and, therefore, changes the modal interference pattern. Note that this shift in modal wavenumbers can alternatively be interpreted as a change in range: a perturbation in the interference is associated with different propagation paths of the modes due to their different group velocities. Clearly, the effect of the source/receiver dynamics is weak for the short ranges but it increases with distance.

Figure 2b demonstrates the combined effects of rough surface scattering and dynamics on the transmission loss as a function of depth (at a fixed range of 100 km). This figure makes clear what is meant by the intensity distribution for the static case (dotted curve) being redistributed as a result of the source/receiver motion (solid curve). Here, a change in the modal interference is evident as well.

Thus, the numerical calculations allow us to conclude that, in spite of slow source/receiver speed, the intensity variations caused by the dynamics can be essential. These variations are especially strong in the range dependence of transmission loss (up to 20 dB).

3.2 Signal Coherence

First, we illustrate the effects of dynamics on the temporal behaviour of the acoustic MCF. Below, we consider only the case where both source and receiver are moving with the same speed and direction.

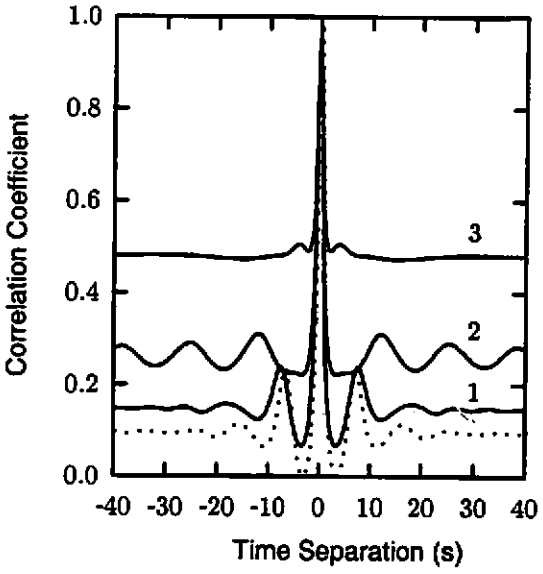

Fig. 3. The normalized MCF of time separation for both moving (solid curves) and for stationary (dotted curve) source and receiver at 30 km range: $1-u=2.5$ m/s, $2-u=5$ m/s, $3-u=10$ m/s

Figure 3 shows a comparison of the MCF of time separation for the dynamic scenario (solid lines) and for the static case (dotted curve). We clearly observe a considerable change in the shape of the temporal correlation coefficient caused by the dynamics. It is evident in Fig. 3 that for the given set of the parameters the level of the residual coherence increases with increasing source/receiver speed. This circumstance is associated with the fact that the modal interference pattern changes differently for each source/receiver speed.

As a second example, we consider the physical manifestation of the receiver motion effect on vertical and horizontal coherence. Now we assume a corresponding receiving array to be stationary, and the source to move away with a speed of 10 m/s from an initial range of 30 km.

The resulting normalized MCF of vertical and horizontal separations is shown in Fig. 4, where the solid curve again represents the dynamic result, and the dashed curve represents the static result. (The origin along the abscissa axis in Fig. 4a is the depth (55 m) of the midpoint of the vertical array). Similarly to the previous case, it is also evident that the "tails" of the spatial MCF are affected essentially by the source dynamics.

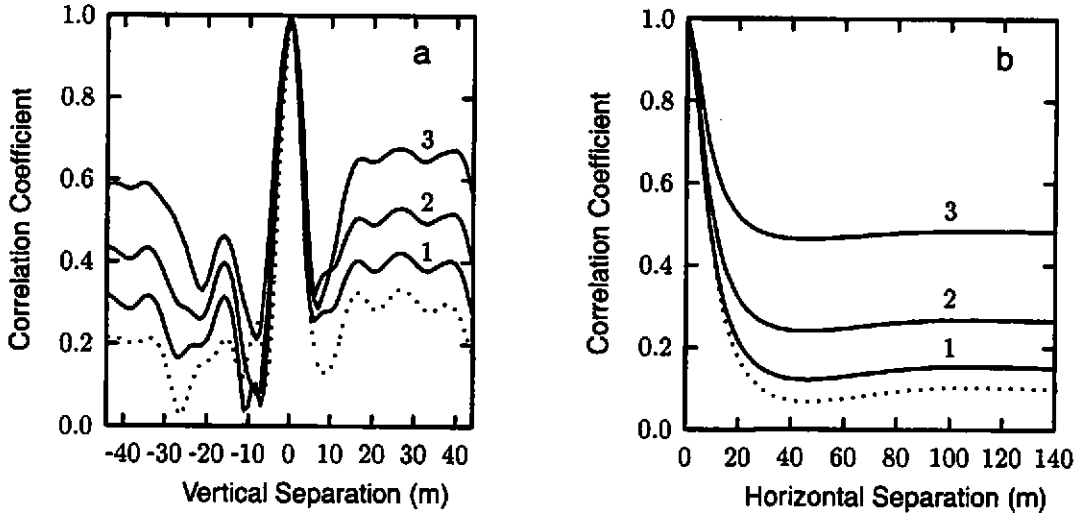

Fig. 4. The normalized MCF of vertical (a) and horizontal (b) separations for source moving away from corresponding array from an initial range of 30 km (solid curves) and for stationary source (dotted curve): $1-u_s=2.5$ m/s, $2-u_s=5$ m/s, $3-u_s=10$ m/s

ACKNOWLEDGMENTS

This work was supported by DERA (United Kingdom) under Grant No SSDW1/918.

REFERENCES

1. M. J. Beran and S. Frankenthal. Volume scattering in a shallow channel. J. Acoust. Soc. Amer., 1992, vol. 91(5), pp. 3203–3211.
2. D. B. Creamer. Scintillating shallow–water waveguides. J. Acoust. Soc. Amer., 1996, vol. 99(5), pp. 2825–2838.
3. M. J. Beran and S. Frankenthal. Combined volume and surface scattering in a channel using a modal formulation. J. Acoust. Soc. Amer., 1996, vol. 100(3), pp. 1463–1472.
4. D. Tielbürger, S. Finette, and S. Wolf. Acoustic propagation through an internal wave field in a shallow water waveguide. J. Acoust. Soc. Amer., 1997, vol. 101(2), pp. 789–808.
5. A. N. Guthrie, R. M. Fitzgerald, D. A. Nutile, and J. D. Schaffer. Long-range low-frequency cw propagation in the deep ocean: Antigua–Newfoundland. J. Acoust. Soc. Amer., 1974, vol. 56(3), pp. 1673–1680.
6. K. E. Hawker. A normal mode theory of acoustic Doppler effects in the oceanic waveguide. J. Acoust. Soc. Amer., 1979, vol. 65(2), pp. 675–681.
7. P. H. Lim and J. M. Ozard. On the underwater acoustic field of a moving point source. I. Range-independent environment. J. Acoust. Soc. Amer., 1994, vol. 95(1), pp. 131–137.
8. H. Schmidt and W. A. Kuperman. Spectral and modal representations of the Doppler-shifted field in ocean waveguides. J. Acoust. Soc. Amer., 1994, vol. 96(1), pp. 386–395.
9. B. J. Uscinski. Performance of horizontal towed arrays. Effect of internal waves. In: *Arrays and Beamforming in Sonar* (Pt. 5, Bristol, 1996), Vol. 18 of *Proceedings of the Institute of Acoustics*, pp. 129–146.
10. F. G. Bass and I. M. Fuks. *Wave Scattering From Statistically Rough Surface* (Pergamon, Oxford, U.K, 1979).
11. B. M. Kudryashov. On the evaluation of acoustic fields in waveguides with statistically rough surface. In: *Mathematical Problems of Geophysics* (Nauka, Novosibirsk, 1973), Vol. 4, pp. 256–272 [in Russian].
12. A. Beilis and F. D. Tappert. Coupled mode analysis of multiply rough surface scattering. J. Acoust. Soc. Amer., 1979, vol. 66(3), pp. 811–826.